

GeSi alloys: A study of short-range order

Bal K. Agrawal

Department of Physics, University of Allahabad, Allahabad, India

(Received 4 January 1980)

A cluster Bethe lattice method has been employed for a study of the effects of short-range order on the electronic and optical properties of binary SiGe alloys. A realistic six-parameter tight-binding parameter Hamiltonian has been used for the study of chemically ordered and random sequences. In random alloys, one observes properties which are simply averages over the properties of the constituent atoms weighted with their concentrations. In chemically ordered alloys, the ionicity manifests itself as a dip in the valence-band electron density of states. The amount of ionicity is proportional to the strength of the dip which increases with the concentration of one constituent in minority to a maximum for a $\text{Si}_{0.5}\text{Ge}_{0.5}$ alloy. One observes an "ionic gap" of width ~ 1.2 eV in the $\text{Si}_{0.5}\text{Ge}_{0.5}$ alloy. This degree of short-range order may be measurable by photoemission experiments. The variation of the band gap with concentration is seen to be in good agreement with the experimental data available for the optical gap in crystalline SiGe alloys. We also observe a small impurity band in the band gap in both sequences except in the $\text{Si}_{0.5}\text{Ge}_{0.5}$ alloy which simulates a zinc-blende-type alloy.

I. INTRODUCTION

The crystalline electronic properties of elemental semiconductors (Ge, Si) are by now quite well understood. There is a negligible electronegativity difference in Ge and Si atoms and one expects a random distribution of atoms in a GeSi alloy. However, the electronic and optical properties of these crystalline and amorphous binary are not well understood. There are some electron energy band calculations in various approximations like a virtual crystal,¹ single site-coherent potential,² and zinc-blende perfect crystal.³ However, all these calculations may be considered merely as linear interpolation schemes between the elemental properties of the constituents of the alloy. The effect of the short-range order (SRO) on the properties has not been studied except in the variational method of Gubanov and Rudenko⁴ where again a random alloy was assumed. Thus a study of the effects of correlations among neighboring atoms on the electronic and optical properties of the simplest available GeSi alloy is very much needed.

Unfortunately, the experimental situation regarding the existence of the degree of SRO in GeSi alloys is not clear. For example, in crystalline GeSi alloys, optical absorption⁵ and p - n junction tunneling⁶ measurements are consistent with a random distribution of the constituents in order to understand the variation of the average phonon frequency involved in the indirect transitions. But the positive heat of formation⁷ and diffuse x-ray scattering⁸ measurements point towards a tendency of clustering of like atoms. In amorphous GeSi alloys the x-ray diffraction⁹ measurements have been understood on the basis of a random alloy. On the other hand, the Raman

spectra results of Lannin¹⁰ have shown need of a theory which includes clustering effects.

The effects of SRO in GeSi alloys has been studied recently by Kittler and Falicov¹¹ using a cluster Bethe-lattice method (CBLM). These authors have considered a simple sp^3 Hamiltonian which includes the nearest-neighbor interactions along the directed bond between sites along with the intra-site interactions. However, there remains a problem of extension of the CBLM to a more realistic Hamiltonian. This is the subject matter of the present paper.

In the present paper we consider a more realistic six-parameter tight-binding Hamiltonian in which all the nearest-neighbor interactions between the s and p orbitals are accounted for. We make a comparison between the electronic density of states for different short-range order and alloy concentrations. Section II contains a brief summary of the interpolation scheme relating to the bond probabilities with the branching ratios of a Bethe lattice. The method of cluster Bethe lattice (CBLM) is applied to a GeSi alloy in Secs. III and IV. The results and their discussion are included in Sec. V.

II. INTERPOLATION SCHEME

In order to relate the bond probabilities to the branching ratios of a Cayley tree, we employ an interpolation scheme used earlier by Kittler and Falicov.¹² A probabilistic description of the local environment of an atom can be formulated in terms of bond probabilities and the concept of valence saturation. For a tetrahedrally coordinated SiGe alloy, the coordination number is four. Let us define the probabilities of the existence of different bonds in an alloy. Let s , $2r$, and g be the

respective probabilities of finding an arbitrary bond between the nearest-neighbor atoms of Si-Si type, Si-Ge or Ge-Si type, and Ge-Ge type. The probabilities should satisfy the normalization condition.

$$s + 2r + g = 1. \quad (1)$$

Let the concentrations of Ge and Si atoms be C and $1 - C$, respectively, and the total numbers of atoms in the solid be N . Each atom has four bonds and each bond is counted twice while summing over all the atoms, so that the total number of nearest-neighbor bonds would be $2N$. Now consider Ge atoms. The total number of Ge-Ge and Ge-Si bonds should saturate all the CN Ge atoms and one gets

$$(2) 2Ng + (2N) 2r = 4CN,$$

i.e.,

$$(g + r) = C. \quad (2)$$

The first term contains an extra factor of 2 because each Ge-Ge bond saturates two Ge atoms. Similarly, for Si atoms one obtains

$$(s + r) = 1 - C, \quad (3)$$

r will be determined by the type of sequence which one desires to consider in a solid. It will take different values for different sequences like segregation, chemically ordered (binary), or random sequences.

The probability parameters may now be used to interpolate the branching ratios of the Cayley tree in the cluster Bethe-lattice method in order to ensure that the same amount of nearest-neighbor correlation is present in the Cayley tree as in the cluster under investigation. In a cluster, let us denote the average number of like-atom nearest-neighbor bonds made by an a (b) atom by P_a (P_b), and the average number of unlike-atom nearest-neighbor bonds by Q_a (Q_b). Here we specify the Ge and Si atoms by a and b , respectively. It is obvious that

$$P_a = \frac{4g}{(g+r)} \equiv \frac{4g}{C}, \quad Q_a = \frac{4r}{(g+r)} \equiv \frac{4r}{C}, \quad (4)$$

$$P_b = \frac{4s}{(s+r)} \equiv \frac{4s}{(1-C)}, \quad Q_b = \frac{4r}{(s+r)} \equiv \frac{4r}{(1-C)}.$$

Let us consider a particular site in the Cayley tree. Its descendants will be determined by the level of the valence saturation already present due to its parent atom. Let P_{ab} (Q_{ab}) be the probability of like (unlike) atom descendants of an a atom having b as its parent atom. The branching ratios of the descendants would be consistent with the saturation condition and the cluster averages for the following values of average probabilities

in the cluster:

$$P_{aa} = P_{ab} = g/C, \quad Q_{aa} = Q_{ab} = r/C, \\ P_{bb} = P_{ba} = s/(1-C), \quad Q_{bb} = Q_{ba} = r/(1-C). \quad (5)$$

Three different sequences may now be chosen for describing the different bonding tendencies.

(i) Segregation sequence: If the like atoms are clustered, we would not have any Ge-Si bond. One may write $r = 0$, $g = C$, and $s = 1 - C$:

$$P_{aa} = P_{bb} = 1, \quad Q_{aa} = Q_{bb} = 0. \quad (6)$$

(ii) Random sequence: Here any kind of atom has equal probability to saturate the valence of an atom compatible with the multiplicities

$$P_a = Q_b \quad \text{and} \quad P_b = Q_a. \quad (7)$$

We thus have

$$g = C^2, \quad r = C(1-C), \quad s = (1-C)^2. \\ P_{aa} = C, \quad Q_{aa} = (1-C), \quad (8)$$

$$P_{bb} = (1-C), \quad Q_{bb} = C.$$

(iii) Chemically ordered or binary sequence: In this sequence atoms of small concentration will try to surround themselves with the atoms of high concentration. Consequently, we have two situations corresponding to $g = 0$ or $s = 0$,

$$(a) \quad g = 0, \quad r = C, \quad \text{and} \quad s = 1 - 2C,$$

$$P_{aa} = 0, \quad Q_{aa} = 1, \quad (9)$$

$$P_{bb} = (1 - 2C)/(1 - C), \quad Q_{bb} = C/(1 - C). \quad (10)$$

$$(b) \quad s = 0, \quad r = (1 - C), \quad \text{and} \quad g = (2C - 1),$$

$$P_{aa} = (2C - 1)/C, \quad Q_{aa} = (1 - C)/C, \quad (11)$$

$$P_{bb} = 0, \quad Q_{bb} = 1. \quad (12)$$

III. CLUSTER BETHE LATTICE

A. Pure lattice

We now consider the evaluation of the Bethe-lattice Green's function for a simple tight-binding Hamiltonian but realistic enough in reproducing a good description of the valence bands of a pure solid. In this nearest-neighbor interaction model, the electrons on each atom are described by one s orbital and three p orbitals (p_x, p_y, p_z). One needs to know six interaction integrals which are parametrized and fitted to crystalline bulk band structures. The interaction integrals are¹³

$$E_s = \langle s | H | s \rangle, \quad E_p = \langle p | H | p \rangle, \\ U = \langle s | H | s' \rangle, \quad V = \langle p_x | H | p'_x \rangle, \quad (13)$$

$$S = \langle s | H | p'_x \rangle, \quad T = \langle p_x | H | p'_y \rangle,$$

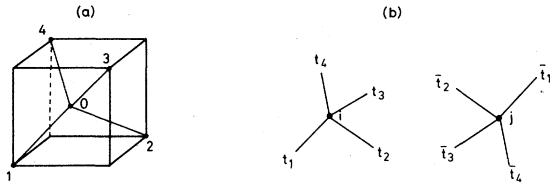


FIG. 1. (a) A lattice site in the tetrahedrally coordinated lattice with its four nearest neighbors. (b) The transfer matrices at the two nearest-neighbor sites.

where the primes on orbitals specify the nearest-neighbor site.

The four nearest neighbors of an atom of a tetrahedrally coordinated lattice are shown in Fig. 1(a). In the Bethe-lattice method one reduces the infinite coupled equations of Green's-function matrix elements to a finite small set of equations involving the transfer matrices (or effective fields).¹⁴

The Dyson equation for the Green's-function matrix may be written as

$$(E\underline{I} - \underline{H}^0)\underline{G} = \underline{I} + \underline{V}\underline{G}, \quad (14)$$

where E is the energy, G is the Green's-function matrix, H^0 is the diagonal matrix for the energies of the noninteracting orbitals at the same site, V is the interaction Hamiltonian matrix between the orbitals lying on the nearest-neighbor sites, and I is the unit matrix.

Equations (14) form an infinite set of coupled equations which can be reduced to a finite set by using the two symmetries of the Bethe lattice. In Fig. 1(b) we represent a four-dimensional vector in the space of orbitals by a dot. In the open structure of Bethe lattice, every dot can be transformed into any other dot by a fixed set of transformation. Also, any two nearest-neighbor dots are connected to each other by only one self-avoiding path. One can thus define a transfer matrix t_ν for each inequivalent line (ν) joining any two nearest-neighbor dots. In Fig. 1(b) we have shown them as t_1, t_2, t_3, t_4 at one site and $\bar{t}_1, \bar{t}_2, \bar{t}_3, \bar{t}_4$ at the neighboring site. The whole lattice is replaced by only one dot interacting with the four transfer matrices. By definition the Green's function at one site should be identically equal to one with the entire Bethe lattice. We

TABLE I. Parameters of the tight-binding Hamiltonian (in eV) for Ge, Si, and GeSi alloys used in the calculation.

Solid	E_s	E_p	U	V	S	T
Ge	-4.29	4.13	-1.70	0.66	1.33	1.71
Si	-2.66	4.54	-2.03	0.79	1.47	1.88
GeSi			-1.87	0.73	1.40	1.80

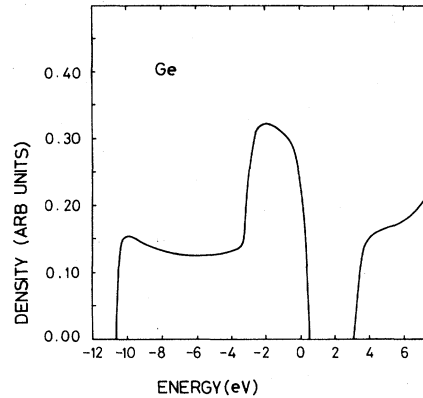


FIG. 2. Electron density of states in amorphous Ge.

may thus write the Green's-function matrix for the site i as

$$\underline{G}_{ii} = (E\underline{I}_i - \underline{H}_{ii}^0 - \underline{F})^{-1},$$

where

$$\underline{F} = \sum_{j=1}^4 \underline{V}_{ij} \underline{t}_{i(j)}, \quad (15)$$

and $\underline{t}_{i(j)}$ denotes the transfer matrix at site i along the direction of atom j . With the requirement that the Green's function \underline{G}_{ii} should be identically equal to one obtained by just taking two dots with the corresponding transfer matrices, one obtains the following two equations for the transfer matrices in a pure solid:

$$\underline{t}_{i(j)} = (E\underline{I}_{jj} - \underline{H}_{jj}^0 - \underline{F} + \underline{V}_{ij}^T \underline{t}_{i(i)})^{-1} \underline{V}_{ij}^T \quad (16)$$

and

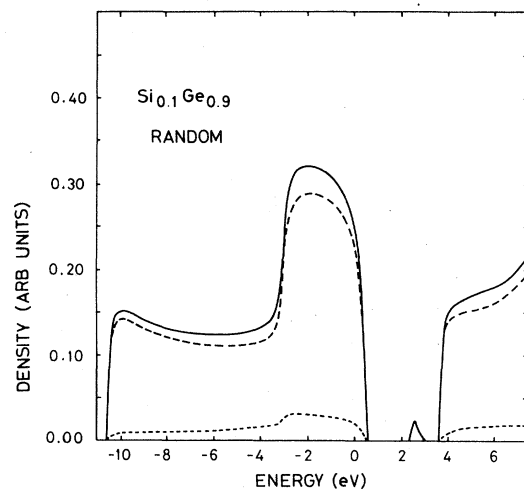


FIG. 3. Electron density of states in an amorphous $\text{Si}_{0.1}\text{Ge}_{0.9}$ alloy in random sequence. The contribution of Si atoms is denoted by the (---) line and that of Ge atoms by the (-·-·-) line. The continuous curve depicts the total density of states.

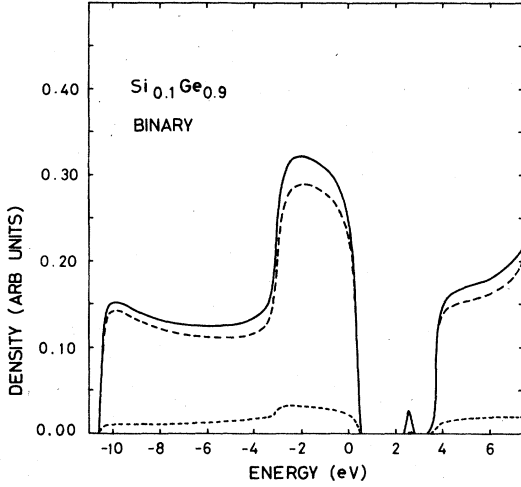


FIG. 4. Same as in Fig. 3 except that the results are for an $\text{Si}_{0.1}\text{Ge}_{0.9}$ alloy in chemically ordered or binary sequence.

$$\bar{t}_{j(i)} = (E\bar{I}_{jj} - \bar{H}_{jj}^0 - \bar{F} + \bar{V}_{ij}t_{i(j)})^{-1}\bar{V}_{ij}. \quad (17)$$

Equations (16) and (17) may be solved for determining the eight transfer matrices t_p and \bar{t}_p . Knowing them, one determines the Green's function (15) at any site. The local density of states at atom i may be obtained from

$$D_i(E) = -(1/\pi) \text{Im Tr} \bar{G}_{ii}. \quad (18)$$

B. GeSi alloy

In a SiGe alloy, equations similar to (16) and (17) may be written for the eight transfer matrices after taking into account the various probabilities of the Ge-Ge, Ge-Si, Si-Ge, and Si-Si bonds. The equations may then be solved numerically

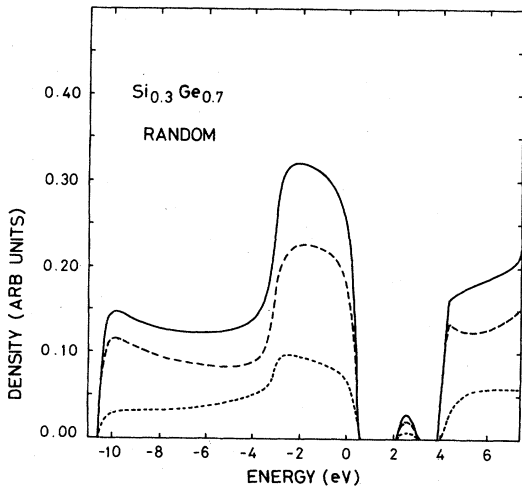


FIG. 5. Same as in Fig. 3 except that the results are for an $\text{Si}_{0.3}\text{Ge}_{0.7}$ alloy in random sequence.

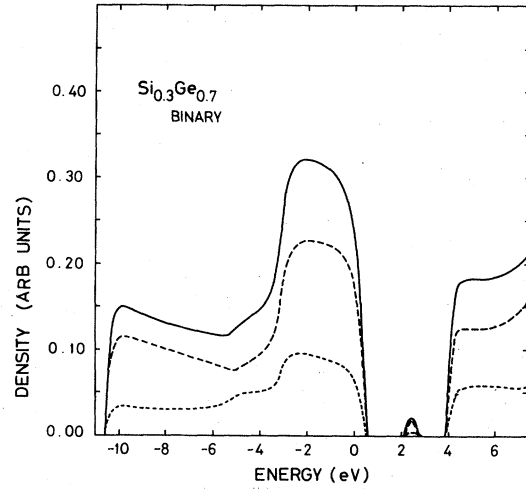


FIG. 6. Same as in Fig. 3 except that the results are for an $\text{Si}_{0.3}\text{Ge}_{0.7}$ alloy in chemically ordered or binary sequence.

by iteration.

In the interpolation scheme employed here, we have four different kinds of sites in the Bethe lattice. The branching ratios at a site are determined by the kind of atom at that particular site and its parent atom. The transfer matrices for a particular site with respect to its parent atom are determined by the kind of bond between them, i.e., Ge-Ge, Ge-Si, Si-Ge, or Si-Si. The equations for an alloy are

$$\begin{aligned} t_1 &= \underline{V}_{aa}(E\underline{I} - \underline{H}_{aa}^0 - P_{aa}\underline{V}_{aa}\bar{t}_1 - Q_{aa}\underline{V}_{ab}\bar{t}_3)^{-1}, \\ \bar{t}_1 &= \underline{V}_{aa}^T(E\underline{I} - \underline{H}_{aa}^0 - P_{aa}\underline{V}_{aa}^T t_1 - Q_{aa}\underline{V}_{ab}^T \bar{t}_3)^{-1}, \\ t_2 &= \underline{V}_{ab}(E\underline{I} - \underline{H}_{aa}^0 - P_{aa}\underline{V}_{aa}\bar{t}_1 - Q_{aa}\underline{V}_{ab}\bar{t}_3)^{-1}, \\ \bar{t}_2 &= \underline{V}_{ab}^T(E\underline{I} - \underline{H}_{aa}^0 - P_{aa}\underline{V}_{aa}^T t_1 - Q_{aa}\underline{V}_{ab}^T \bar{t}_3)^{-1}, \\ t_3 &= \underline{V}_{ba}(E\underline{I} - \underline{H}_{bb}^0 - P_{bb}\underline{V}_{bb}\bar{t}_4 - Q_{bb}\underline{V}_{ba}\bar{t}_2)^{-1}, \\ \bar{t}_3 &= \underline{V}_{ba}^T(E\underline{I} - \underline{H}_{bb}^0 - P_{bb}\underline{V}_{bb}^T t_4 - Q_{bb}\underline{V}_{ba}^T \bar{t}_2)^{-1}, \\ t_4 &= \underline{V}_{bb}(E\underline{I} - \underline{H}_{bb}^0 - P_{bb}\underline{V}_{bb}t_4 - Q_{bb}\underline{V}_{ba}t_2)^{-1}, \\ \bar{t}_4 &= \underline{V}_{bb}^T(E\underline{I} - \underline{H}_{bb}^0 - P_{bb}\underline{V}_{bb}^T \bar{t}_4 - Q_{bb}\underline{V}_{ba}^T \bar{t}_2)^{-1}. \end{aligned} \quad (19)$$

The local Green's functions at the two constituent atoms may be written as

$$\begin{aligned} \underline{G}_{aa} &= (E\underline{I} - \underline{H}_{aa}^0 - \frac{1}{3}P_{aa}\underline{V}_{aa}t_1 - \frac{1}{3}Q_{aa}\underline{V}_{ab}\bar{t}_3)^{-1}, \\ \underline{G}_{bb} &= (E\underline{I} - \underline{H}_{bb}^0 - \frac{1}{3}P_{bb}\underline{V}_{bb}\bar{t}_4 - \frac{1}{3}Q_{bb}\underline{V}_{ba}\bar{t}_2)^{-1}. \end{aligned} \quad (20)$$

The superscript T denotes the transpose of the matrix. The total density of states is the sum over the four orbitals at the central atom of a five-atom cluster which is averaged over all the possible cluster configurations consistent with the short-range order assumed. The contribution of each constituent atom towards the electronic

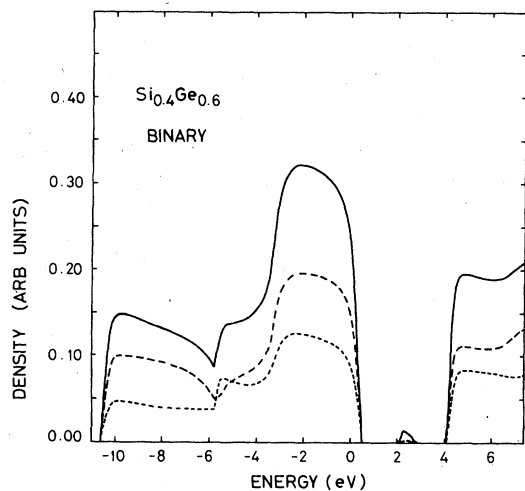


FIG. 7. Same as in Fig. 3 except that the results are for an $\text{Si}_{0.4}\text{Ge}_{0.6}$ alloy in chemically ordered or binary sequence.

density of the solid would be proportional to its concentration in the solid.

IV. CALCULATION

In order to have any numerical result, one has to make a choice of the tight-binding parameters for pure Ge and Si and their alloy. For Ge and Si, we employ the parameters determined by Chadi and Cohen.¹⁵ The relative positions of the *s* and *p* orbitals for Ge and Si atoms are taken similar to Kittel and Falicov.¹¹ As no reliable values of the interaction parameters for Ge-Si or Si-Ge bonds are available, we have made the simplest choice, i.e., we take the averages of the interaction parameters of the constituent atoms

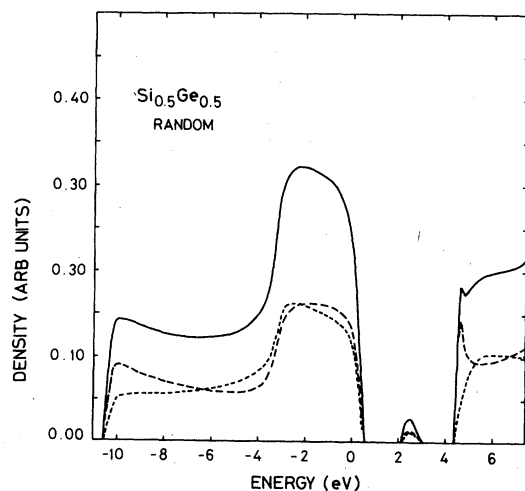


FIG. 8. Same as in Fig. 3 except that the results are for an $\text{Si}_{0.5}\text{Ge}_{0.5}$ alloy in random sequence.

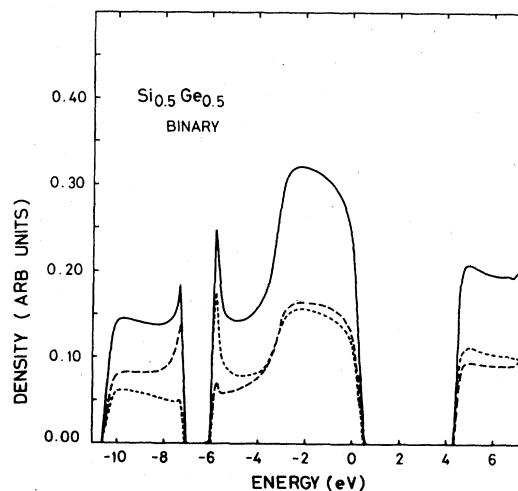


FIG. 9. Same as in Fig. 3 except that the results are for an $\text{Si}_{0.5}\text{Ge}_{0.5}$ alloy in chemically ordered or binary sequence.

to simulate them for the alloy. The values of the different parameters used in the calculation are given in Table I.

Equations (19) were solved for various concentrations of the constituents by iteration. The calculations have been performed for the binary and random sequences and the results are presented in Figs. 2-15. In these figures the relative contributions of the constituent atoms have also been depicted. Figures 2 and 15 depict the density of states in the pure materials.

The variation of the semiconductor energy gap with concentration is found to be similar for both the sequences. This variation is shown in Fig. 16. For comparison we reproduce the experi-

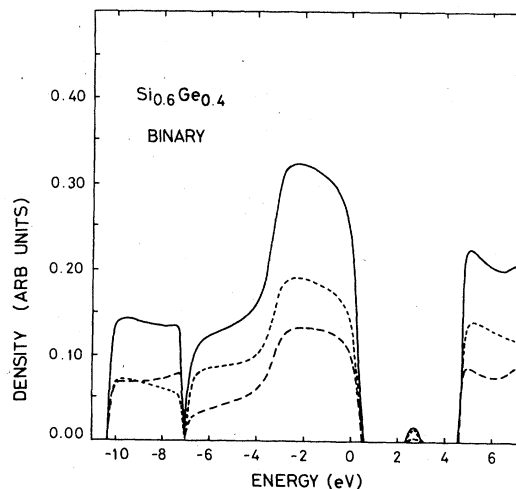


FIG. 10. Same as in Fig. 3 except that the results are for an $\text{Si}_{0.6}\text{Ge}_{0.4}$ alloy in chemically ordered or binary sequence.

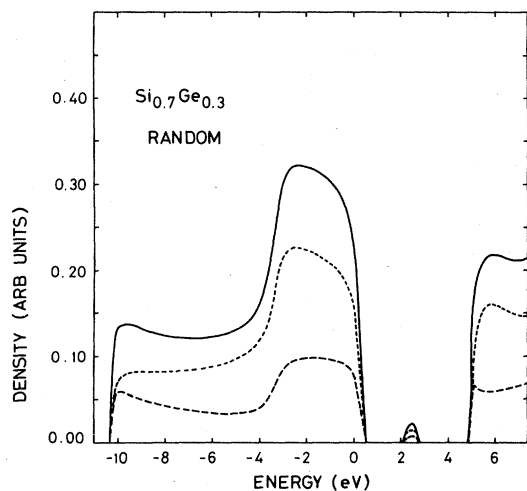


FIG. 11. Same as in Fig. 3 except that the results are for an $\text{Si}_{0.7}\text{Ge}_{0.3}$ alloy in random sequence.

mental data of Kline *et al.*¹⁶ for the optical gap in crystalline GeSi alloys as well as the earlier results of Kittler and Falicov¹¹ for the band gap.

V. RESULTS AND DISCUSSION

In random alloys we observe average properties in proportion to the concentrations of the constituent Ge and Si atoms. However, in chemically ordered or binary alloys, we observe the effects of ionicity. At any concentration the manifestation of ionicity in separating the two regions corresponding to Ge and Si atoms is determined by the amount of correlation in the alloy. An actual ionic gap opens up only for a 40% concentration of Ge atoms. In a $\text{Ge}_{0.5}\text{Si}_{0.5}$ alloy, we find a gap of width ~ 1.2 eV

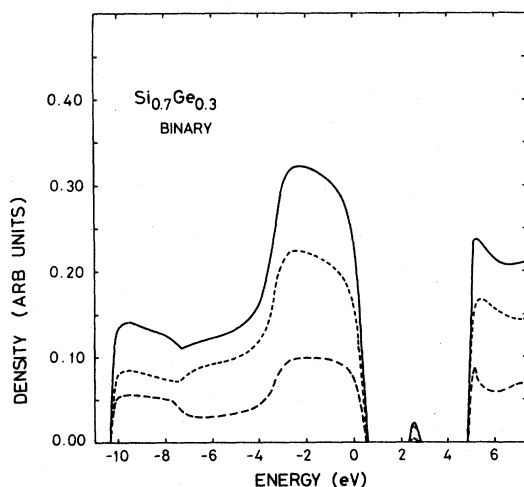


FIG. 12. Same as in Fig. 3 except that the results are for an $\text{Si}_{0.7}\text{Ge}_{0.3}$ alloy in chemically ordered or binary sequence.

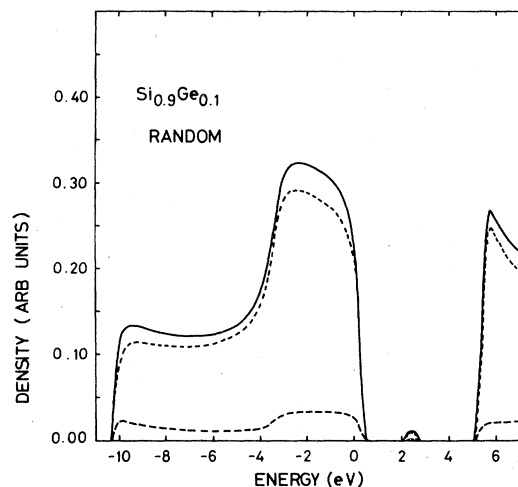


FIG. 13. Same as in Fig. 3 except that the results are for an $\text{Si}_{0.9}\text{Ge}_{0.1}$ alloy in random sequence.

which is nearly equal to that obtained by Stukel⁸ (~ 1.1 eV) in a ZnS-type crystal structure of SiGe. However, the amount of ionicity manifests itself as the area of the dip in the binary sequence. For very small concentrations of one constituent this dip is quite small. The strength of the dip increases with the concentration up to the $\text{Si}_{0.5}\text{Ge}_{0.5}$ alloy, where one observes a full ionic gap, and then decreases until a pure Ge is reached. These dips should be observable in the photoemission experiments and one may measure the degree of SRO in alloys. The variation of the ionic gap with concentration is shown in Fig. 17.

In both sequences there appears a weak band in the band gap in the energy range 2.0–3.0 eV,

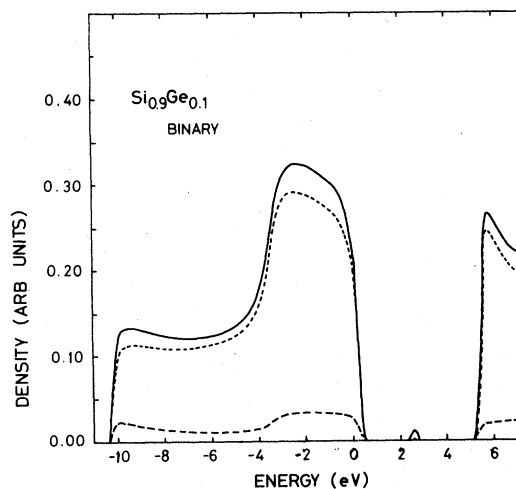


FIG. 14. Same as in Fig. 3 except that the results are for an $\text{Si}_{0.9}\text{Ge}_{0.1}$ alloy in chemically ordered or binary sequence.

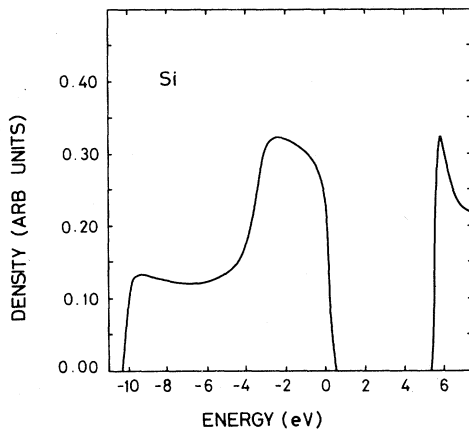


FIG. 15. Electron density of states in amorphous Si.

except in the case of $\text{Ge}_{0.5}\text{Si}_{0.5}$ alloy in the binary sequence, where the alloy simulates a perfect zinc-blende structure. Also, the band does not appear in pure Ge and Si. The total density of states in this band increases with the concentration of minority atoms reaching to a maximum for nearly equal concentrations of the constituent

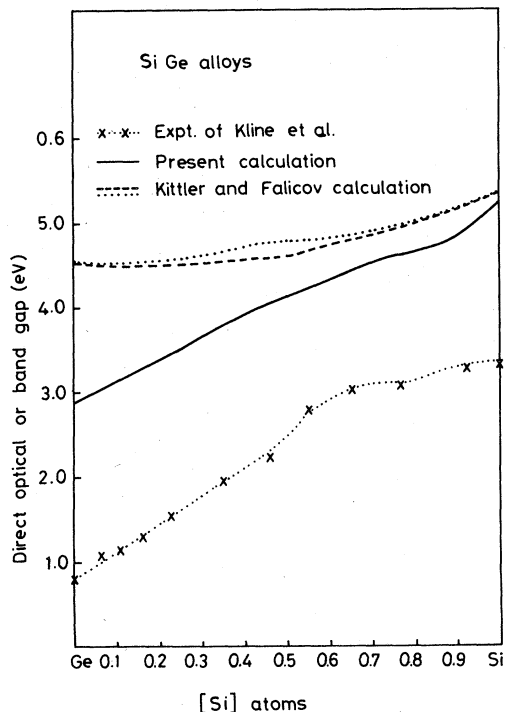


FIG. 16. Variation of the band gap or optical gap with concentration in GeSi alloys. The solid curve denotes the present results for the band gap. The calculated band gaps of Kittler and Falicov (Ref. 11) for the binary and random sequences are shown by (···) and (----) curves, respectively. The experimental points of Kline *et al.* (Ref. 16) for the minimum optical gap at each concentration are depicted by (x-x-x).

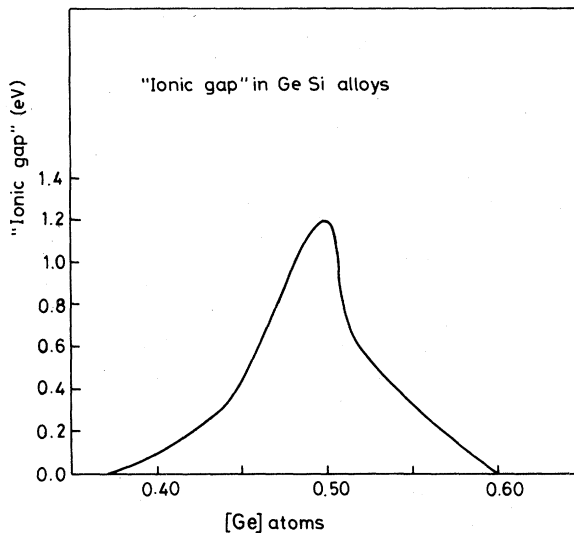


FIG. 17. Variation of ionic gap with Ge concentration.

atoms. The impurity band seems to arise from the alloying.

The measurements of Kline *et al.* reveal¹⁶ a linear dependence of several direct optical gaps on concentration in GeSi alloys. If we assume that the variation of the *smallest* direct optical gap with concentration is similar to that of band gap in the present calculation, we may derive the concentration dependence. In Fig. 16 this dependence is depicted and compared with the experimental points. We observe a negligible departure from linearity, i.e., only a small bowing in the band gap. Also, we observe a concentration dependence which is similar in random and binary sequences. These results are different from those of Kittler and Falicov¹¹ who have seen large and different bowings in random and binary sequences. Although the form of the variation of the band gap with concentration is in good agreement with experiment, there arises an almost constant difference of ~ 1.9 eV between the calculated and the experimental values over most of the concentration range. It arises in part from the smaller bandwidth of the Bethe lattice and can be corrected by changing the interaction parameters in the lattice.¹⁷

ACKNOWLEDGMENTS

The author is thankful to the Science Research Council of the United Kingdom for financial support. He is grateful to Professor J. L. Beeby for hospitality and to Professor E. A. Davis for his suggestions concerning comparison with the experimental data. This work was supported in part by the Centre Nationale Recherche Scientifique, Paris, when the author was at the Laboratory of the Study of Surfaces and Interfaces, I. S. E. N., 3 rue F. Baes, Lille, France.

- ¹F. Bassani and D. Brust, *Phys. Rev.* **131**, 1524 (1963).
²D. J. Stroud and H. Ehrenreich, *Phys. Rev. B* **2**, 3197 (1970).
³D. J. Stukel, *Phys. Rev. B* **3**, 3347 (1971).
⁴A. I. Gubanov and V. G. Rudenko, *Fiz. Tekh. Poluprovodn.* **5**, 1547 (1971) [*Sov. Phys.—Semicond.* **5**, 1351 (1972)].
⁵R. Braunstein, A. R. Moore, and F. Herman, *Phys. Rev.* **109**, 695 (1958).
⁶R. A. Logan, J. M. Powell, and F. A. Trumbore, *Phys. Rev.* **136**, 1751 (1964).
⁷J. P. Dismukes, L. Ekstrom, and R. Paff, *J. Phys. Chem.* **68**, 3021 (1964).
⁸Ya. S. Umanskii, V. I. Prilepskii, and S. S. Gorelik, *Fiz. Tverd. Tela (Leningrad)* **7**, 2673 (1965) [*Sov. Phys.—Solid State* **7**, 2162 (1966)].
⁹N. J. Shevchik, J. S. Lannin, and J. Tejada, *Phys. Rev. B* **7**, 3987 (1973).
¹⁰J. S. Lannin, *Phys. Rev. B* **16**, 1510 (1977).
¹¹R. C. Kittler and L. M. Falicov, *J. Phys. C* **10**, 1667 (1977).
¹²R. C. Kittler and L. M. Falicov, *J. Phys. C* **9**, 4259 (1976).
¹³J. C. Slater and G. F. Koster, *Phys. Rev.* **94**, 1498 (1954).
¹⁴J. D. Joannopoulos, *Phys. Rev. B* **16**, 2764 (1977).
¹⁵D. J. Chadi and M. L. Cohen, *Phys. Status Solidi B* **68**, 405 (1975).
¹⁶J. S. Kline, F. H. Polk, and M. Cardona, *Helv. Phys. Acta* **41**, 968 (1968).
¹⁷J. D. Joannopoulos and F. Yndurain, *Phys. Rev. B* **10**, 5164 (1974).